*Research Article*

# A Prediction Algorithm for Coexistence Problem in Multiple-WBAN Environment

## Zilong Jin,[1] Yoonjeong Han,[1] Jinsung Cho,[1] and Ben Lee[2]

[1]*Department of Computer Engineering, Kyung Hee University, Yongin 446-701, Republic of Korea*
[2]*School of Electrical Engineering and Computer Science, Oregon State University, Corvallis, OR 97331, USA*

Correspondence should be addressed to Jinsung Cho; chojs@khu.ac.kr

The coexistence problem occurs when a single wireless body area network (WBAN) is located within a multiple-WBAN environment. This causes WBANs to suffer from severe channel interference that degrades the communication performance of each WBAN. Since a WBAN handles vital signs that affect human life, the detection or prediction of coexistence condition is needed to guarantee reliable communication for each sensor node of a WBAN. Therefore, this paper presents a learning-based algorithm to efficiently predict the coexistence condition in a multiple-WBAN environment. The proposed algorithm jointly applies PRR and SINR, which are commonly used in wireless communication as a way to measure the quality of wireless connections. Our extensive simulation study using Castalia 3.2 simulator based on the OMNet++ platform shows that the proposed algorithm provides more reliable and accurate prediction than existing methods for detecting the coexistence problem in a multiple-WBAN environment.

## 1. Introduction

A wireless body area network (WBAN) is a human-centered network providing communication among devices that exist in/on/around a human body. IEEE 802.15 Working Group organized IEEE 802.15 Tasking Group 6 in 2007 to establish the standardization for WBANs with the aim of simultaneously providing services for medical and entertainment applications [1].

Due to the limited bandwidth, the performance of WBANs suffers when multiple users occupy the same channel at the same time, referred to as the *coexistence problem*. This also causes received signal strength to decrease reducing channel capacity. As a result, packet error rate (PER) increases and packet reception ratio (PRR) decreases. PER is defined as the ratio of the number of incorrectly transferred data packets, where a packet is assumed to be incorrect if at least one bit is incorrect, and the total number of transmitted packets. On the other hand, PRR is the ratio of the number of received packets and the number of transmitted packets. Therefore, the coexistence problem increases retransmissions and delay, which decrease the channel utilization rate. Thus,

it is important to avoid the coexistence problem by predicting it beforehand.

There are a number of algorithms that detect the coexistence problem based on estimating *signal to interference plus noise ratio* (SINR) [2–5]. However, estimating SINR using RF transceivers is inaccurate because of errors introduced by the analog circuitry. Therefore, these methods cannot accurately detect the coexistence condition. Furthermore, they neglect the fact that WBANs are human-centric networks. This means that the wireless environment changes frequently with users' mobility and postural movement, and thus prediction algorithms based on instantaneous estimation of SINR are not reliable.

This paper proposes a learning-based method for predicting the coexistence condition in a multiple-WBAN environment. The learning-based algorithm is used to become aware of changes in the wireless environment and to improve the accuracy of the prediction algorithm. The proposed algorithm jointly applies PRR and SINR, which are commonly used in wireless communication to measure the quality of wireless connections. The learning process can be performed based on supervised and unsupervised learning methods

which perform learning tasks with labeled and unlabeled data, respectively. Due to the huge complexity and low estimation accuracy, unsupervised learning methods cannot accomplish the estimation task efficiently in tiny sensor based networks such as wireless sensor networks and wireless body area networks. On the other hand, supervised learning algorithms are easily applied to WBAN because it performs the learning task based on the labeled training data and provides relatively high accuracy with low algorithm complexity [6, 7]. There are several supervised learning methods, for example, neural network, decision tree, and naive-Bayesian classifier. This paper employs the naive-Bayesian classifier because it has relatively low computational complexity and classifies the coexistence condition into four states: *Static*, *Semidynamic*, *Dynamic*, and *None*. (The specific learning process will be discussed in Section 3.)

The performance of the proposed method is compared with existing techniques using simulations. Our study shows that the proposed algorithm provides more reliable and accurate prediction performance than existing methods to detect the coexistence condition in a multiple-WBAN environment.

The rest of this paper is organized as follows. Section 2 provides the state of the art and the background related to the proposed method. The proposed prediction algorithm is presented in Section 3. Section 4 discusses the performance evaluation of the proposed algorithm. Finally, Section 5 concludes the paper and discusses future work.

## 2. Related Work and Background

*2.1. Related Work.* The coexistence problem has been actively researched for WBANs, which require high transmission reliability. There are a number of studies on the performance degradation of a WBAN in a multiple-WBAN environment [8, 9]. However, these studies only measure performance and do not provide an efficient detection or prediction schemes for the coexistence situation.

There are also studies on detection or prediction of the coexistence problem based on wireless transmission technologies, such as wireless local area networks (WLANs) and wireless personal area networks (WPANs). These existing studies target different communication layers. At the physical (PHY) layer, interference is detected prior to transmission, which is the most accurate way to check whether or not a channel is occupied by other users. However, a WBAN requires low power consumption and thus detecting signal power is not viable [10]. A number of methods [2, 3] use SINR or bit error rate (BER) to detect interference. However, an accurate judgment cannot be made with only a single SINR value because it may contain errors. Detecting whether or not received signal strength indicator (RSSI) exceeds a threshold is another way to check if interference exists. RSSI is useful for detecting interference between devices using different types of communication technologies that have a wide variation in signal power, for example, Bluetooth and WLAN [11]. At the medium access control (MAC) layer, PER is the criterion for detecting interference [12]. Finally, packet delivery rate (PDR) is used at the network layer. However, prediction of

coexistence based on a single measured value at the MAC or the network layer is not reliable. Therefore, a reliable coexistence prediction model that considers interference characteristics at each layer is required for WBANs.

Due to the aforementioned limitations of the existing methods, this paper aims to provide an algorithm that jointly considers PRR and SINR to improve the accuracy of predicting the coexistence problem. In order to make the prediction algorithm robust to changes in the wireless environment, a learning-based scheme is applied to detect the coexistence condition based on measured PRR and SINR values.

*2.2. Naive-Bayesian Classifier.* Machine learning techniques are regarded as efficient solutions to improve the performance of adaptive algorithms by learning the patterns of specific factors. Supervised and unsupervised learning methods are particular cases that perform learning tasks with labeled and unlabeled data, respectively. Due to the huge algorithm complexity and low estimation accuracy, unsupervised learning methods cannot efficiently perform the estimation task in wireless networks. On the other hand, supervised learning algorithms are widely applied to wireless networks to estimate the variance of wireless resources and network environment [6, 7].

The naive-Bayesian classifier, which is based on the Bayes rule, is a widely used supervised learning method that exploits posterior probability calculation with a priori information. It performs the classification by counting the number of examples; therefore, it can provide relatively low computational complexity compared with the other supervised learning methods (e.g., neural network and decision tree) and can be easily deployed in sensor devices.

The naive-Bayesian classifier, $c_{\text{MAP}}$, can be used to estimate the most possible hypothesis based on existing feature variables and is defined as follows:

$$
\begin{aligned}
c_{\text{MAP}} &= \arg\max_{c_j \in C} \frac{P(w_1, w_2, \ldots, w_n \mid c_j) P(c_j)}{P(w_1, w_2, \ldots, w_n)} \\
&= \arg\max_{c_j \in C} P(w_1, w_2, \ldots, w_n \mid c_j) P(c_j),
\end{aligned}
\tag{1}
$$

where $c_j$ indicates the class within the class space $C$ and $w_1, w_2, \ldots, w_n$ represent the feature variables. When the feature variables are assumed to be conditionally independent, the result of (1) can be calculated as $P(w_1, w_2, \ldots, w_n \mid c_j)P(c_j) = \prod_i P(w_i \mid c_j)$. Substituting this into (1), the naive-Bayes classifier can be obtained as follows:

$$
c_{\text{MAP}} = \arg\max_{c_j \in C} P(c_j) \prod_i P(w_i \mid c_j).
\tag{2}
$$

The prior probabilities $P(w_i \mid c_j)$ in (2) can be obtained by looking at how often each class appears in the training data set. After calculating the posterior probabilities of the classes, the maximum a posteriori (MAP) hypothesis selects the class $c_j$ for which the computation is the maximum.
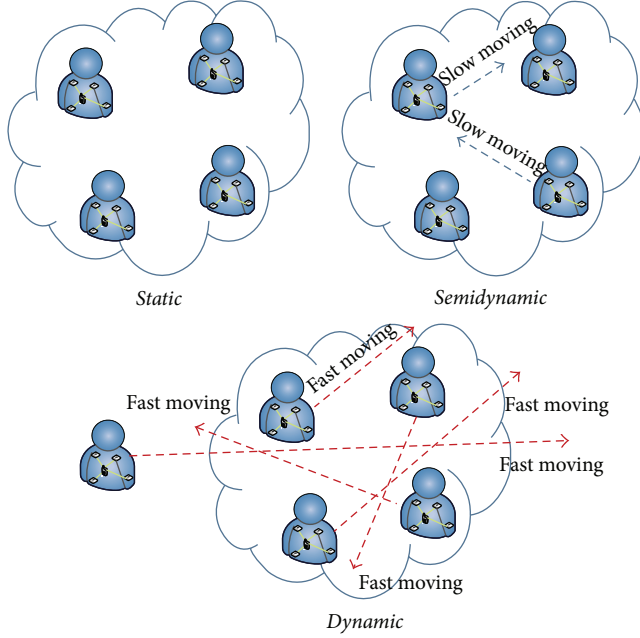
FIGURE 1: Multiple-WBAN environment.

TABLE 1: IEEE Std. 802.15.6 defined coexistence environment.

| | |
|---|---|
| Static | A single WBAN in a residential environment or a hospital with a single patient node and a fixed bedside hub |
| Semidynamic | Slowly moving ambulatory patients in an elderly care facility |
| Dynamic | Fast moving ambulatory patients in a hospital with a large number of WBANs |

## 3. Proposed Algorithm

This section discusses the proposed learning algorithm based prediction scheme that can provide high prediction accuracy for the coexistence states.

*3.1. System Model and Problem Description.* Figure 1 shows the different multiple-WBAN environments, where each WBAN has a different moving speed and in turn influences the duration of the coexistence problem to other WBANs. IEEE Std. 802.15.6 classifies the coexistence condition based on the mobility level shown in Table 1. However, the standard does not clearly define the parameters, such as moving speed, that distinguish among these three states. Therefore, based on IEEE Std. 802.15.6, this paper quantitatively defines the coexistence states of *Static*, *Semidynamic*, and *Dynamic* scenarios using the *time duration of interference*, $T_{SINR}$, which indicates the duration of time when SINR value is lower than or equal to a threshold value $SINR_{th}$. (It will be given by a set of experiences in the following subsection.)

More specifically, the coexistence states are defined as follows.

(i) *Static* (S) state indicates that there is a constant interference from other WBANs for a period with

```
input: PRR, SINR, T_SINR, Pre-state PRR_th, SINR_th  α, β
output: State
(1)  if PRR ≥ PRR_th  then
(2)       PRR = True
(3)  else
(4)       PRR = False
(5)  if SINR ≥ SINR_th  then
(6)       T_SINR = 0
(7)       else if  T_SINR > 0 && T_SINR < α  then
(8)            T_SINR = 1
(9)       else if  T_SINR ≥ α && T_SINR < β  then
(10)           T_SINR = 2
(11)      else if  T_SINR ≥ β  then
(12)           T_SINR = 3
(13) end
(14) State = NBClassifier (PRR, T_SINR, Pre-state)
(15) return State
```

PSEUDOCODE 1: Pseudocode for overall flow of the proposed scheme.

no mobility (the definition for time threshold will be given in the following section).

(ii) *Semidynamic* (SD) state indicates that there is a constant interference from other WBANs for a period with slow mobility.

(iii) *Dynamic* (D) state indicates that there is a temporary interference from other WBANs with fast mobility.

(iv) *None* (N) state indicates that there is no interference.

PRR and SINR are utilized as the classification feature variables for interference detection, and the coordinator node calculates average PRR and SINR values of received packets from the sensor nodes. $T_{SINR}$ is measured and used to classify the coexistence condition instead of the instantaneous SINR value. Furthermore, we assume that the *Previous-state* has an influence on the current state in addition to PRR and $T_{SINR}$. Consequently, our aim is to detect the coexistence problem in a multiple-WBAN environment by applying the three measured values, which are PRR, $T_{SINR}$, and *Previous-state*, to the naive-Bayesian classifier and classifying the coexistence condition into the four states defined in Table 1.

Pseudocode 1 shows the pseudocode for the proposed scheme. First, the average PRR value is compared with the PRR *threshold* ($PRR_{th}$). (It will be given by a set of experiences in the following subsection.) There are two possible results which may be greater or less than ($PRR_{th}$). Therefore, PRR value is converted into a Boolean variable for simply applying in naive-Bayesian classifier. Then, the average SINR value is compared with the SINR threshold ($SINR_{th}$). If it is greater than the threshold, according to the definition of $T_{SINR}$, there is no time duration that satisfies $SINR \leq SINR_{th}$; thus $T_{SINR}$ is set to 0. Otherwise, $T_{SINR}$ is compared with the time boundary of $\alpha$ and $\beta$ ($\alpha < \beta$), which are the bounds for evaluating the characteristics of coexistence states and obtained through experiments. After comparison, the value of $T_{SINR}$ is converted to integer values $\{1, 2, 3\}$ representing the interval in which it is included. Finally, PRR, $T_{SINR}$, and *Previous-state*,

TABLE 2: Training data.

| PRR | SINR | *Previous-state* | Current state |
|---|---|---|---|
| PRR ≥ PRR$_{\text{th}}$ | $T_{\text{SINR}} = 0$ | N | N |
| | | S | |
| | | SD | |
| | | D | |
| | $0 < T_{\text{SINR}} < \alpha$ | N | D |
| | | SD | |
| | | D | |
| | $\alpha \leq T_{\text{SINR}} < \beta$ | N | D |
| | | SD | |
| | | D | |
| | $\beta \leq T_{\text{SINR}}$ | N | N |
| | | S | |
| | | SD | |
| | | D | |
| PRR < PRR$_{\text{th}}$ | $T_{\text{SINR}} = 0$ | N | N |
| | | S | |
| | | SD | |
| | | D | |
| | $0 < T_{\text{SINR}} < \alpha$ | N | D |
| | | SD | |
| | | D | |
| | $\alpha \leq T_{\text{SINR}} < \beta$ | N | SD |
| | | SD | |
| | | D | |
| | $\beta \leq T_{\text{SINR}}$ | N | S |
| | | S | |
| | | SD | |
| | | D | |

which may be one of *None*, *Static*, *Semidynamic*, or *Dynamic* states, are fed to the naive-Bayesian classifier, which returns the state with the highest posterior probability.

*3.2. Training Data and Prior Probability.* In the naive-Bayesian classifier, the classification algorithm needs to be trained with a set of training data. In general, the training data can be obtained from intuitive knowledge or accumulation of experiential information. In this paper, a set of experiments is performed for a variety of WBAN environments to obtain the labeled training data. These experiments are performed using ZigbeX II modules running an embedded OS and equipped with the CC2420 transceiver. For the implementation of a multiple-WBAN environment, a WBAN consisting of one coordinator node and four sensor nodes is interfered by sensor nodes belonging to the other WBANs.

The labeled training data is obtained using experiments and is shown in Table 2. For example, the labeled training data for the second row is obtained when PRR ≥ PRR$_{\text{th}}$ and $0 < T_{\text{SINR}} < \alpha$, and this condition has three possible previous states: *None* (N), *Semidynamic* (SD), and *Dynamic* (D). For these particular feature values, the current coexistence state is *Dynamic*. Thus, the labeled training data can be used to

compute the prior probabilities of each of the coexistence state, and then the most likely state can be chosen.

The coordinator node calculates average PRR based on the number of dropped and received packets from the four sensor nodes. The number of dropped packets can be obtained by checking the sequence number of received packets. In addition, the coordinator node calculates average SINR based on measurements taken from the four sensor nodes using the equation shown below:

$$\text{SINR} = 10 \log_{10} \frac{10^{\text{RSS}/10} - 10^{n/10}}{10^{\text{RIS}/10}}, \tag{3}$$

where RSS is the average received signal strength from the sensor nodes and RIS is the received interference signal strength from other WBANs and $n$ is the noise level measured at the coordinator node. $T_{\text{SINR}}$ can then be recorded when the calculated SINR value is lower than or equal to SINR$_{\text{th}}$.

In order to generate the training data, we performed experiments for four types of interference cases. In the first case, there is no interference in order to evaluate the *None* state. In the second case, there is a fixed interfering node that affects the WBAN's communication in order to evaluate the *Static* state. In the third and fourth cases, the interfering node moves at 0.5 m/s (slow) and 1.5 m/s (fast) to evaluate the *Semidynamic* and *Dynamic* states, respectively. Each case is performed 5 times and then average PRR and $T_{\text{SINR}}$ values are recorded.

The experimental results for different coexistence conditions are shown in Figure 2. *None 1* and *None 2* represent the results for the first case, where the transmission rate of *None 2* is two times higher than *None 1*. *Dynamic 1* and *Dynamic 2* represent the fourth case, where the interfering node of *Dynamic 2* is closer to the subject WBAN than *Dynamic 1*. These experimental results show that the current state can be derived based on the previous measured data and exhibit the following characteristics.

(i) *Static* state: Figure 2(b) shows that average SINR values are relatively stable and less than 0 dBm. Therefore, $T_{\text{SINR}}$ is relatively large in this state. At the same time, average PRR values are low (~70%) as shown in Figure 2(a). Therefore, the current state can be *Static* only when PRR < PRR$_{\text{th}}$ and $T_{\text{SINR}}$ is greater than time bound of $\beta$. (According to our experiment, $\beta$ is set to an appropriate value of 19 s.)

(ii) *Semidynamic* state: Figure 2(a) shows that average PRR value is lower than 90%. Moreover, average value of SINR is less than SINR$_{\text{th}}$ from 3 s to 7.5 s. Therefore, the *Semidynamic* state is possible only when PRR < PRR$_{\text{th}}$ and $T_{\text{SINR}}$ is greater than a time duration bound $\alpha$ (where $\alpha = 3$ s).

(iii) *Dynamic* state: Figure 2(a) shows that PRR values may be higher or lower than PRR$_{\text{th}}$ = 90%. Moreover, when PRR < PRR$_{\text{th}}$, the time duration, $T_{\text{SINR}}$, when SINR value is less than SINR$_{\text{th}}$ is less than $\alpha$. On the other hand, when PRR > PRR$_{\text{th}}$, $T_{\text{SINR}}$ values can be less or greater than $\alpha$ as shown in Figure 2(b). Therefore, the *Dynamic* state is possible when PRR and
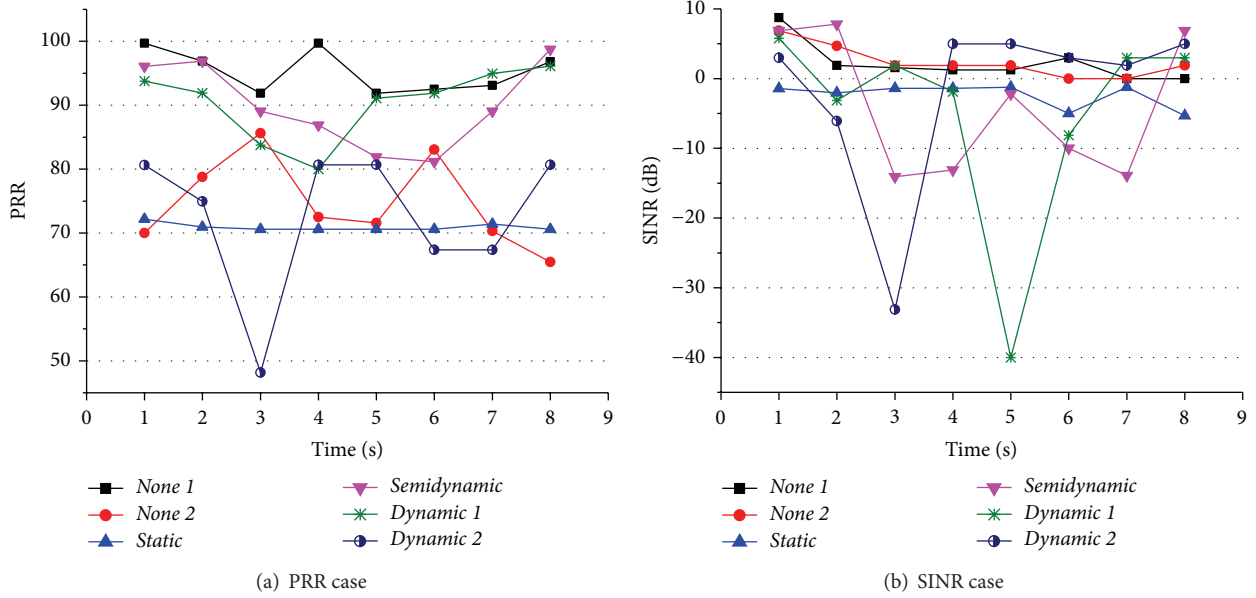
(a) PRR case



(b) SINR case

FIGURE 2: Average PRR and SINR values according to the coexistence condition.

$T_{SINR}$ satisfy PRR < $PRR_{th}$ and $T_{SINR}$ < $\alpha$ or PRR > $PRR_{th}$ and $T_{SINR}$ < $\beta$.

(iv) *None* state: Figure 2(a) shows that PRR values may be higher or lower than $PRR_{th}$ = 90%. Furthermore, since there is no interference in *None* state, SINR ≥ $SINR_{th}$ as shown in Figure 2(b). When SINR > $SINR_{th}$, $T_{SINR}$ = 0 because there is no time duration that satisfies SINR ≤ $SINR_{th}$. When SINR = $SINR_{th}$, $T_{SINR}$ may tend to be large (when a patient stays in a ward where there is few interfering wireless devices for long time). Therefore, the *None* state is possible when PRR > $PRR_{th}$ and $T_{SINR}$ < $\alpha$ or $T_{SINR}$ > $\beta$, and PRR < $PRR_{th}$ and $T_{SINR}$ < $\alpha$.

Therefore, the training data used to classify the current state in Table 2 can be obtained from analyzing PRR and $T_{SINR}$ values in Figure 2.

*3.3. Naive-Bayesian Classifier Application.* The naive-Bayesian classifier defined in (2) accepts the measured values PRR, $T_{SINR}$, and *Previous-state* as the feature variables and computes the probability of each state based on the training data. For example, when the measured values indicate PRR ≥ $PRR_{th}$, 0 < $T_{SINR}$ < $\alpha$, and *Previous-state* = N, the probability that the current state is *Static* is given by the following calculation:

$$P(S) \cdot P\left(PRR \geq PRR_{th} \mid S\right) \cdot P\left(0 < T_{SINR} < \alpha \mid S\right)$$
$$\cdot P(N \mid S) = \frac{4}{28} \times 0 \times 0 \times \frac{1}{4} = 0. \quad (4)$$

More specifically, the probability that the current state is *Static* $P(S)$ = 4/28 is obtained by counting the number of examples of the state *Static* that are in the training data and

dividing by the total number of the training data. Under the given condition of *Static*, the a priori probability of $P(PRR \geq PRR_{th} \mid S)$ and $P(0 < T_{SINR} < \alpha \mid S)$ is 0 and $P(N \mid S)$ is 1/4. Therefore, $P(S \mid PRR \geq PRR_{th}, 0 < T_{SINR} < \alpha, N)$ = 0, and, thus, the probability that the current state is *Static* is 0.

Similarly, the probabilities that the current states are *Semidynamic*, *Dynamic*, and *None* are calculated as follows:

$$P(SD) \cdot P\left(PRR \geq PRR_{th} \mid SD\right) \cdot P\left(0 < T_{SINR} < \alpha \mid SD\right)$$
$$\cdot P(N \mid SD) = \frac{3}{28} \times 0 \times 0 \times \frac{1}{3} = 0,$$
$$P(D) \cdot P\left(PRR \geq PRR_{th} \mid D\right) \cdot P\left(0 < T_{SINR} < \alpha \mid D\right)$$
$$\cdot P(N \mid D) = \frac{9}{28} \times \frac{6}{9} \times \frac{6}{9} \times \frac{3}{9} = \frac{1}{21},$$
$$P(N) \cdot P\left(PRR \geq PRR_{th} \mid N\right) \cdot P\left(0 < T_{SINR} < \alpha \mid N\right)$$
$$\cdot P(N \mid N) = \frac{12}{28} \times \frac{8}{12} \times 0 \times \frac{3}{12} = 0.$$
$$(5)$$

Based on these results, *Dynamic* is chosen as the most likely state for the current state.

## 4. Performance Evaluation

*4.1. Simulation Model.* This section presents our simulation study using the OMNeT++ platform, which is a modular simulation library for studying wired and wireless communication networks, to evaluate the performance of the proposed algorithm. In our simulation environment, a single WBAN consists of one coordinator node and four sensor nodes

TABLE 3: Predicted coexistence state per speed.

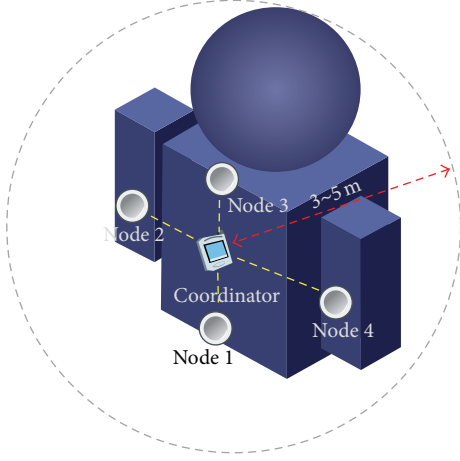| | Case 1 | | Case 2 | | Case 3 | | Case 4 | |
| --- | --- | --- | --- | --- | --- | --- | --- | --- |
| | Speed (m/s) | Coexistence state | Speed (m/s) | Coexistence state | Speed (m/s) | Coexistence state | Speed (m/s) | Coexistence state |
| R1 | 0.2 | SD | 0.4 | D | 0.2 | SD | 0.2 | SD |
| R2 | 0.2 | SD | 0.4 | D | 0 | S | 0.4 | D |
| R3 | 0 | S | 0.2 | D | 0.4 | D | 0 | D |
| R4 | 0.4 | N | 0.2 | N | 0.4 | D | 0.2 | D |
| R5 | 0.4 | D | — | — | 0.2 | N | 0.4 | D |



FIGURE 3: A single WBAN.

(i.e., Node 1, Node 2, Node 3, and Node 4), which are located 1 m from the coordinator node as shown in Figure 3.

In a WBAN, PRR is calculated by the coordinator node based on the average number of received packets from the four sensor nodes. SINR is obtained from RSS measurements taken directly from the four sensor nodes using (3) as described in Section 3.2, and then $T_{SINR}$ value is obtained by recording the time duration of SINR which is less than $SINR_{th}$.

In the simulation, all nodes use CC2420 transceiver that operates in the 2.4 GHz frequency band and the transmit power is fixed at −3 dBm. The packet transmit rate is set to 10 pkts/s and 5 pkts/s, and $PRR_{th}$ and $SINR_{th}$ are 90% and 0 dBm, respectively, to guarantee good communication quality. Finally, we set $\alpha = 3$ and $\beta = 19$ based on the experimental results and Table 2 in Section 3.2.

Figure 4 shows our simulation environment, which reflects the situations where multiple WBANs exist in the same area. There are 19 WBANs in the simulation area of 24 m × 16 m. Due to the fact that mobility is relative, the subject WBAN (M-BAN1) is mobile while the other 17 WBANs (BAN3–BAN17) are static and act as interfering WBANs. Moreover, in order to provide a more general simulation environment, another mobile interfering WBAN, M-BAN2, is introduced to simulate interference from mobile as well as static WBANs. The simulation area is subdivided into six 8 m × 8 m regions, which are indicated as R1–R6 in Figure 4,

and different densities of WBANs are deployed to different regions. In regions R1 and R4, there is no static interference. On the other hand, the subject M-BAN1 suffers from high interference in region R3 and low interference in regions R2 and R5. The region R6 is used to record the initial *Previous-state*.

In order to evaluate the performance of the proposed algorithm for various types of interference, four simulation cases are tested based on the moving speeds of M-BAN1 and the interference node density. Case 1 and Case 2 have 17 fixed interfering WBANs, and Case 3 and Case 4 have 17 fixed interfering WBANs and one mobile interfering M-BAN2. The subject M-BAN1 moves along the path shown in red at speeds of 0 m/s, 0.2 m/s, and 0.4 m/s. On the other hand, static interfering WBANs are positioned at fixed locations indicated by dots, and the mobile interfering M-BAN2 moves along the path shown as a dotted red line at 0.4 m/s. While the subject M-BAN1 moves, the coordinator node gathers information and calculates the current values of PRR and $T_{SINR}$ and records *Previous-state*.

Table 3 shows the different moving speeds of M-BAN1 for the four cases, and the correct coexistence state is labeled based on moving speeds of M-BAN1 and interference density. For example, the data in the first row, first column (i.e., 0.2 m/s), indicates the moving speed of M-BAN1 in region R1. During this time, M-BAN1 experiences low interference and its moving speed is slow; thus the correct state is *Semidynamic*.

*4.2. Simulation Result.* The coordinator of M-BAN1 measures average PRR and $T_{SINR}$ values, as well as *Previous-state,* when it communicates with its sensor nodes in regions R1–R5, which are shown in Table 4. For example, the first row for Case 1 indicates that PRR = 0.981, $T_{SINR}$ = 3 s, and *Previous-state* is *Dynamic*, and Table 3 shows that the moving speed of M-BAN1 in R1 is 0.2 m/s and the actual coexistence state is *Semidynamic*.

Based on analyzing the simulation data shown in Table 4, we find that even though the value of PRR is sensitive to M-BAN1's moving speed, it does not reflect the interference characteristic. For example, the data in the second row of Table 4 shows that PRR increases significantly as moving speed increases from 0.2 m/s to 0.4 m/s for Case 1 and Case 2. This is also similar for Case 3 and Case 4. However, it is difficult to distinguish the coexistence states by comparing just the PRR value for Case 1 and Case 3, where the correct states are *Semidynamic* and *Static*, respectively.
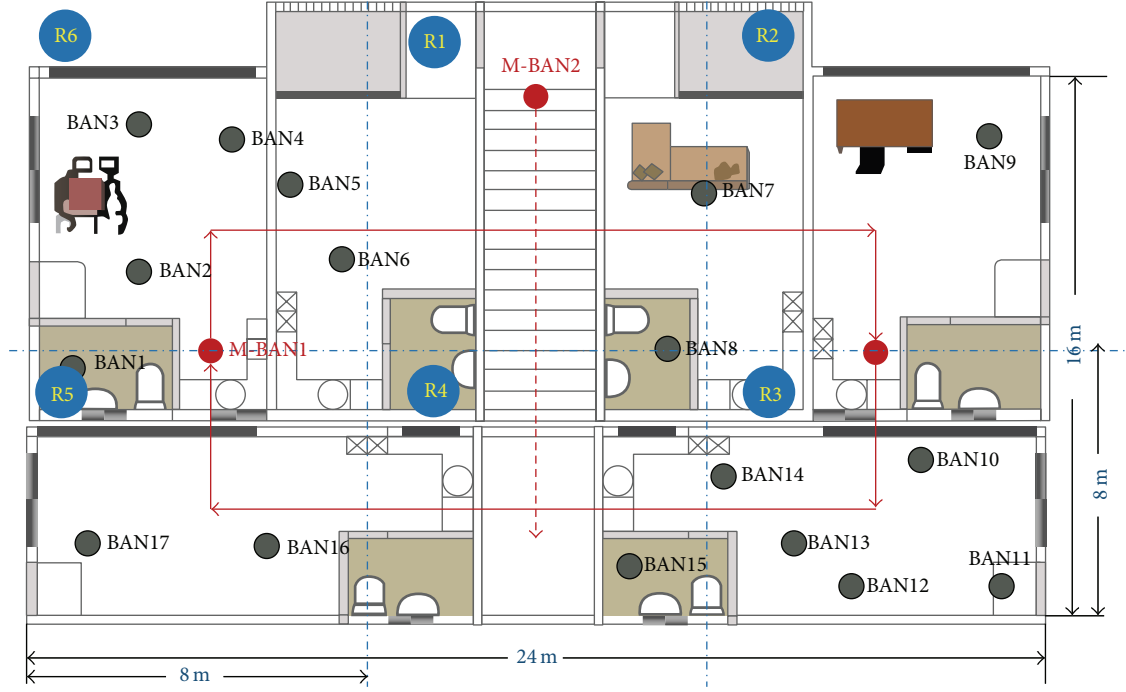
FIGURE 4: Simulation area.

TABLE 4: Simulation results of PRR and $T_{SINR}$.

| | Case 1 | | | Case 2 | | | Case 3 | | | Case 4 | | |
|---|---|---|---|---|---|---|---|---|---|---|---|---|
| | *Previous-state* | PRR (pts/s) | $T_{SINR}$ (s) | *Previous-state* | PRR (pts/s) | $T_{SINR}$ (s) | *Previous-state* | PRR (pts/s) | $T_{SINR}$ (s) | *Previous-state* | PRR (pts/s) | $T_{SINR}$ (s) |
| R1 | D | 0.981 | 3 | D | 0.982 | 5.5 | D | 0.869 | 3 | D | 0.869 | 3 |
| R2 | S | 0.868 | 18 | D | 0.982 | 2 | SD | 0.857 | 20 | SD | 0.982 | 6 |
| R3 | S | 0.807 | 20 | SD | 0.95 | 4 | S | 0.96 | 6 | S | 0.935 | 6 |
| R4 | S | 1 | 0 | N | 1 | 0 | SD | 0.972 | 3.5 | S | 0.972 | 1.5 |
| R5 | N | 0.982 | 2 | — | — | — | D | 1 | 0 | SD | 0.982 | 2 |

Table 5 compares the predicted states using PRR, $T_{SINR}$, and the proposed algorithm against the actual coexistence states for all four cases. The prediction results based on PRR shows that it can be used to check whether or not interference exists, but it does not accurately predict the actual coexistence state. On the other hand, using $T_{SINR}$ leads to a more precise prediction performance than PRR. In Case 1, the coexistence condition can be precisely analyzed based on $T_{SINR}$. For Case 2, $T_{SINR}$ is maintained for a long time in region R2 despite the fact that the subject WBAN is moving at a relatively high speed of 0.4 m/s. In Case 3 and Case 4, M-BAN2 is added. According to the PRR and $T_{SINR}$ values in region R3 for Case 3 and region R2 for Case 4, the predicted coexistence states are *None* and *Semidynamic*, respectively. However, Table 5 shows that the actual state is *Dynamic*, and the proposed algorithm correctly predicts the actual states. Similarly, the PRR and $T_{SINR}$ values in R3 for Case 4 are influenced by the interfering mobile WBAN (i.e., M-BAN2), and the predicted coexistence

states are *None* and *Semidynamic*, respectively, but Table 5 shows that the actual state is *Dynamic*.

In summary, Table 5 shows that the accuracy is 69% when prediction is performed using a single value of $T_{SINR}$. However, when PRR, $T_{SINR}$, and *Previous-state* are jointly considered and applied to the proposed prediction algorithm, the accuracy is 100%.

## 5. Conclusion

This paper proposed a prediction algorithm for detecting the coexistence problem by applying PRR, $T_{SINR}$, and *Previous-state* to a naive-Bayesian classifier to predict the performance of a multiple-WBAN environment. In addition to detecting types of interference, this study plays a major role in attempting to classify coexistence conditions into *Dynamic*, *Semidynamic*, *Static*, and *None* states. Our simulation study shows that the proposed algorithm provides significantly

TABLE 5: Performance result.

(a) Case 1

|      | Actual state | PRR | $T_{\text{SINR}}$ | Proposed algorithm |
| --- | --- | --- | --- | --- |
| R1 | SD | N | SD | SD |
| R2 | SD | D | SD | SD |
| R3 | S | D | S | S |
| R4 | N | N | N | N |
| R5 | D | N | D | D |

(b) Case 2

|      | Actual state | PRR | $T_{\text{SINR}}$ | Proposed algorithm |
| --- | --- | --- | --- | --- |
| R1 | D | N | SD | D |
| R2 | D | N | SD | D |
| R3 | D | N | D | D |
| R4 | N | N | N | N |

(c) Case 3

|      | Actual state | PRR | $T_{\text{SINR}}$ | Proposed algorithm |
| --- | --- | --- | --- | --- |
| R1 | SD | D | SD | SD |
| R2 | S | D | S | S |
| R3 | D | N | SD | D |
| R4 | D | N | D | D |
| R5 | N | N | N | N |

(d) Case 4

|      | Actual state | PRR | $T_{\text{SINR}}$ | Proposed algorithm |
| --- | --- | --- | --- | --- |
| R1 | SD | D | SD | SD |
| R2 | D | N | SD | D |
| R3 | D | N | SD | D |
| R4 | D | N | SD | D |
| R5 | D | N | D | D |

higher reliability in detecting the coexistence conditions compared to existing studies that consider either PRR or SINR. As a future work, we plan to develop suitable handling mechanisms for the coexistence states and evaluate their effectiveness by experiments in a real multiple-WBAN environment.

## Conflict of Interests

The authors declare that there is no conflict of interests regarding the publication of this paper.

## Acknowledgment

## References

[1] IEEE 802.15.6 WPAN Task Group 6 BAN, March 2015, http://www.ieee802.org/15/pub/TG6.html.

[2] E. G. Villegas, E. López-Aguilera, R. Vidal, and J. Paradells, "Effect of adjacent-channel interference in IEEE 802.11 WLANs," in *Proceedings of the 2nd International Conference on Cognitive Radio Oriented Wireless Networks and Communications (CrownCom '07)*, pp. 118–125, August 2007.

[3] D. Fan, X. Wang, and P. Mi, "Cross-layer interference minimization-oriented channel assignment in IEEE 802.11 WLANs," in *Proceedings of the 22nd IEEE International Symposium on Personal, Indoor and Mobile Radio Communications (PIMRC '11)*, pp. 1083–1087, Toronto, Canada, September 2011.

[4] S. C. Liu, G. L. Xing, H. W. Zhang et al., "Passive interference measurement in Wireless Sensor Networks," in *Proceedings of the 18th IEEE International Conference on Network Protocols (ICNP '10)*, pp. 52–61, October 2010.

[5] J. Huang, S. Liu, G. Xing, H. Zhang, J. Wang, and L. Huang, "Accuracy-aware interference modeling and measurement in wireless sensor networks," in *Proceedings of the 31st International Conference on Distributed Computing Systems (ICDCS '11)*, pp. 172–181, July 2011.

[6] S. Ahmed and S. S. Kanhere, "A Bayesian routing framework for delay tolerant networks," in *Proceedings of the IEEE Wireless Communications and Networking Conference (WCNC '10)*, pp. 1–6, Sydney, Australia, April 2010.

[7] S. Marsland, *Machine Learning An Algorithmic Perspective*, Chapman & Hall, New York, NY, USA, 2009.

[8] M. Deylami and E. Jovanov, "Performance analysis of coexisting IEEE 802.15.4-based health monitoring WBANs," *Proceedings of the Annual International Conference of the IEEE Engineering in Medicine and Biology Society (EMBC '12)*, vol. 2012, pp. 2464–2467, 2012.

[9] R. Kazemi, R. Vesilo, and E. Dutkiewicz, "A novel genetic-fuzzy power controller with feedback for interference mitigation in wireless body area networks," in *Proceedings of the IEEE 73rd Vehicular Technology Conference (VTC '11)*, pp. 1–5, May 2011.

[10] Q. Pang and V. C. M. Leung, "Channel clustering and probabilistic channel visiting techniques for WLAN interference mitigation in bluetooth devices," *IEEE Transactions on Electromagnetic Compatibility*, vol. 49, no. 4, pp. 914–923, 2007.

[11] C. Won, J.-H. Youn, H. Ali, H. Sharif, and J. Deogun, "Adaptive radio channel allocation for supporting coexistence of 802.15.4 and 802.11b," in *Proceedings of the 62nd IEEE Vehicular Technology Conference (VTC '05)*, vol. 4, pp. 2522–2526, 2005.

[12] D. G. Yoon, S. Y. Shin, W. H. Kwon, and H. S. Park, "Packet error rate analysis of IEEE 802.11b under IEEE 802.15.4 interference," in *Proceedings of the IEEE 63rd Vehicular Technology Conference (VTC '06)*, pp. 1186–1190, July 2006.